Strong out-of-plane magnetic anisotropy in ion irradiated anatase TiO2 thin films

M. Stiller, J. Barzola-Quiquia, P. Esquinazi, D. Spemann, J. Meijer, M. Lorenz, and M. Grundmann

Citation: AIP Advances **6**, 125009 (2016); doi: 10.1063/1.4971794
View online: http://dx.doi.org/10.1063/1.4971794
View Table of Contents: http://aip.scitation.org/toc/adv/6/12
Published by the American Institute of Physics

Strong out-of-plane magnetic anisotropy in ion irradiated anatase TiO_2 thin films

M. Stiller,[1,a] J. Barzola-Quiquia,[1] P. Esquinazi,[1] D. Spemann,[2,b] J. Meijer,[2] M. Lorenz,[3] and M. Grundmann[3]
[1]*Division of Superconductivity and Magnetism, Institute for Experimental Physics II, University of Leipzig, 04103 Leipzig, Germany*
[2]*Division of Nuclear Solid State Physics, Institute for Experimental Physics II, University of Leipzig, 04103 Leipzig, Germany*
[3]*Semiconductor Physics Group, Institute for Experimental Physics II, University of Leipzig, 04103 Leipzig, Germany*

(Received 21 July 2016; accepted 23 November 2016; published online 7 December 2016)

The temperature and field dependence of the magnetization of epitaxial, undoped anatase TiO_2 thin films on $SrTiO_3$ substrates was investigated. Low-energy ion irradiation was used to modify the surface of the films within a few nanometers, yet with high enough energy to produce oxygen and titanium vacancies. The as-prepared thin film shows ferromagnetism which increases after irradiation with low-energy ions. An optimal and clear magnetic anisotropy was observed after the first irradiation, opposite to the expected form anisotropy. Taking into account the experimental parameters, titanium vacancies as di-Frenkel pairs appear to be responsible for the enhanced ferromagnetism and the strong anisotropy observed in our films. The magnetic impurities concentrations was measured by particle-induced X-ray emission with ppm resolution. They are ruled out as a source of the observed ferromagnetism before and after irradiation. [http://dx.doi.org/10.1063/1.4971794]

I. INTRODUCTION

Since the discovery of defect-induced magnetism (DIM) in different materials above room temperature, e.g. in graphite,[1] several oxide systems or SiC,[1] a new line of research in the study of room temperature ferromagnetism (FM) started for nominally non-magnetic semiconductors, which is a matter of current research.[2–7] The observed FM at such high temperatures is unusual because of the large spin polarization of the, mainly, valence (hole) bands (e.g., O-2p in oxides or the σ band in carbon-based materials) induced by a relatively low defect density of ~ 5 %. The induced FM above room temperature in wide-band gap semiconductors has a large potential for applications in optoelectronics and magneto-optic devices.[8] There is no general consensus, whether cations or anions vacancies are responsible for the magnetic ordering in oxides. For example, studies on HfO_2 or ZrO_2 suggest that the observed FM is due to O vacancies,[9–12] in disagreement with first principle theoretical studies which indicate that O vacancies do not show any magnetic moment in simple, binary oxides, but Hf vacancies do.[3] The observed FM in undoped oxide nanoparticles (Al_2O_3, In_2O_3, ZnO or SnO_2) was attributed to oxygen vacancies at the surface of the particles.[13] Experimental and theoretical studies on the undoped oxide systems such as ZnO[14–16] or TiO_2,[17] indicate that cation vacancies are responsible for stable magnetic moments, which can induce ferromagnetic order[3] when their concentration is around 5 %.[1,15,16]

[a]markus@mstiller.org
[b]Current address: Physic Department, Leibniz Institute for Surface Modification, Permoserstr. 15, 04318 Leipzig, Germany

There are several studies on DIM in TiO_2,[7,18–22] with ferromagnetic signals up to 880 K,[20,23] also for thin films of anatase and rutile prepared by pulsed laser deposition.[24] Several mechanisms have been proposed to explain the source of FM in these materials. According to some band structure calculations,[20] the exchange interaction between Ti^{3+} and Ti^{4+} in anatase can cause FM. However, X-ray photoelectron spectroscopy results, on $TiO_{2-\delta}$ thin films grown on Si substrates under different oxygen pressures, do not find these ions.[24] Results for annealed polycrystalline rutile and rutile/anatase $TiO_{2-\delta}$ powders suggest oxygen vacancies as source for FM. However, only Ti^{4+} vacancies were detected and any exchange mechanism with Ti^{3+} or Ti^{2+} was excluded.[25] In as-grown $Ti_{0.905}O_2$ anatase thin films, Ti vacancies were found to cause ferromagnetism and *p*-type conductivity.[26] In addition, for 4 MeV Ar^{5+} irradiated polycrystalline rutile, Ti vacancies were suggested to be the main source of the room temperature FM[27] and a first principle study found a ferromagnetic moment of 3.5 μ_B per Ti vacancy and 2.0 μ_B per titanium divacancy, oxygen vacancies were excluded as source of a magnetic moment.[28]

Special scientific research interest lies in materials showing perpendicular magnetic anisotropy, due to potential applications such as ultrahigh density magnetic recording,[29] where it is useful to extend the superparamagnetic limit to higher bit densities,[30] or tunnel magnetoresistance junctions.[31] A pure magnetic patterning, without modification of the surface using additional ferromagnetic materials, is highly desirable for future applications. Thus, DIM with out-of-plane anisotropy can be a powerful tool to modify the magnetic properties of samples such as thin films or multilayered structures. Combined with lithography processes, it is possible to pattern ferromagnetic structures. Such magnetic patterns with out-of-plane magnetic anisotropy were produced with low-energy He^+ irradiation in CoPt,[32] SiC[33] and FePd.[34] Increasing the ion fluence, the out-of-plane saturation field and the out-of-plane contribution to the magnetization decreased.[34,35] Out-of-plane magnetic domain structures have also been found in $La_{0.67}Sr_{0.33}MnO_3$ on $SrTiO_3$, where the anisotropy is due to in-plane tensile strain in LSMO film caused by the STO substrate.[36]

In this work, the influence of the irradiation of low-energy ions (maximum energy: ≈ 300 eV) on the magnetic properties of anatase TiO_2 thin films grown on $SrTiO_3$ (STO) was investigated. The low-energy used implies that defects are created only within a few nanometers from the surface of the thin film and to avoid any possible extra magnetic contribution due to modification of the substrate. In addition, low-energy irradiation is more accessible for industrial applications, due to the complication in producing ions with MeV energy, and costly devices. To verify that no magnetic dopants are introduced during growth and treatment with ions, laterally resolved particle-induced X-ray emission (PIXE) was used. The results show that FM is induced by ion irradiation with a Curie temperature above 300 K, and that the responsible defects are not oxygen vacancies but Ti-divacancies. One interesting outcome obtained in this work is the evident magnetic anisotropy observed after the first irradiation, indicating an easy axis parallel to the *c*-axis of the thin film, i.e. normal to the main surface. This magnetic anisotropy vanishes with increasing defect density.

II. EXPERIMENTAL

Here, the experimental procedures are discussed. Section II A describes the thin film production, impurity analysis and magnetization measurements. The details of the used low-energy irradiation are discussed in Section II B, to show the reader how one can estimate the mean free path of different ions that are produced in the plasma and accelerated towards the sample surface.

A. Thin film preparation, impurity analysis and magnetization measurements

The thin films have been prepared using pulsed laser deposition (PLD). As substrate, STO (100) etched by hydrofluoric acid and annealed in oxygen atmosphere prior to the film deposition has been used, which has been shown to be suitable for growing epitaxial anatase thin films.[37] The films have been grown at a temperature of 650°C. The oxygen pressure during the PLD was kept at 0.003 mbar, and the resulting thickness of the film was $\approx$ 150 nm.[37] A sketch of the substrate and sample is shown in FIG. 1. During the growth process, a mask was used to fix the substrates on the holder. As a consequence, the substrate is not completely covered with TiO_2, as sketched in FIG. 1.

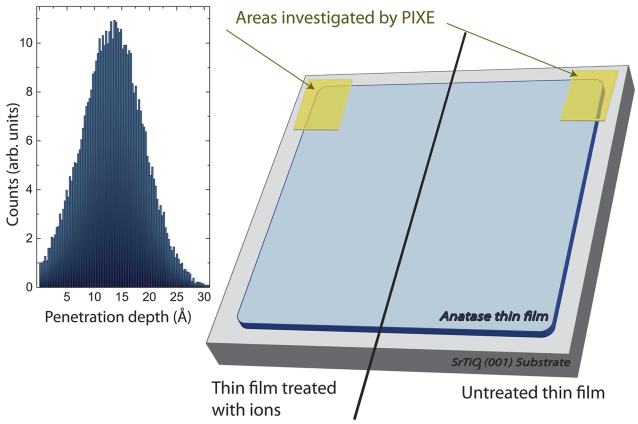

FIG. 1. Sketch of the anatase thin film on the $SrTiO_3$ substrate. During ion irradiation the right side was covered with Teflon. In order to check for impurities, particle-induced X-ray emission measurements were performed on both sides, indicated by yellow areas. The inset shows a SRIM simulation of the penetration depth of the Ar ions (peak value is ≈1.5 nm).

The steps necessary to keep the sample in place, as well as its handling and the process of ion irradiation in the argon/hydrogen plasma chamber, are possible sources of contamination. To check the contribution of contaminants (in particular the magnetic ones) quantitatively, PIXE measurements were performed. This is a very sensitive (accurate) method to measure the main magnetic contaminants in the TiO_2 thin film samples investigated here, with a minimum detection limit of ≈ 6 μg/g. To check for possible contamination during the ion irradiation, 50 % of the sample was covered with Teflon in order to maintain the sample in the as-prepared conditions, see FIG. 1. After treatment, PIXE measurements in both regions (without the Teflon cover) were done as shown in FIG. 1, where the investigated areas are indicated as yellow, transparent squares. The areas were intentionally chosen so that a part of the substrate, a part of the edge of the thin film and the film itself were analyzed. In this way, one obtained information about the contamination of the substrate (due to the growth process and hydrofluoric etching), of the edge of the film (due to the mask used to fix the substrate during the growth process), and of the TiO_2 film as grown, and after the plasma treatment. To further rule out magnetic contamination due to handling or irradiation, a substrate was placed for 1.5 h into the plasma chamber; no measurable change of the magnetic moment was observed. To elucidate the crystallographic structure of the grown TiO_2 thin films, X-ray diffraction (XRD) was performed (Philips X'Pert Diffractometer with Bragg-Brentano goniometer). The field dependence of the magnetic moment at three different temperatures, the temperature dependence of the magnetization at constant applied fields (zero-field and field cooled curves) and the remanence of the sample were measured by a superconducting quantum interference device (SQUID) magnetometer from Quantum Design.

B. Low-energy ion irradiation

The ion irradiation was done in a DC argon/hydrogen plasma chamber with a parallel plate configuration at room temperature using a Ar/H gas mixture (90% Ar and 10% H, Air Liquide). The substrate was placed on a sample holder ≃ 12 cm away from the electric field region, produced by two capacitance plates, where the gas was ionized. The film was connected to ground and the current was measured in order to calculate the amount of irradiated ions. A bias voltage of 300 V is applied to accelerate the ions towards the sample.

The produced plasma consists of 10 different species: e^-, Ar atoms, fast and metastable Ar, ArH^+, H^+, H_2^+, H_3^+, H atoms and H_2 molecules.[38] In our experiment, only the species, which are accelerated towards the sample are of significance. Neutral atoms and molecules are not accelerated by the electric field but exhibit diffusive motion across the chamber. When no electric field was applied, no effects on the magnetic properties and also no change in the impurity concentration were measured. Note that the sample was placed ≃ 12 cm away from the plasma center. The influence of sputtered Cu from

the parallel plates was also ruled out by means of PIXE measurements, see Section III. Therefore, only the in-the-plasma produced ion species and their energy, to estimate the corresponding defect production, were taken into account.

Whether a vacancy can be produced or not, depends on the energy E_{PKA} transferred from the incident ion to the primary knock-on atom (PKA) as follows:[39]

$$E_{\mathrm{PKA}}(d) = E_i \frac{m_1}{m_2}\left[\frac{2m_2}{m_1+m_2}\sqrt{1-\left(\frac{d}{r_1+r_2}\right)^2}\right]^2, \tag{1}$$

where E_i is the ion energy, m_j and r_j are the masses and radii of particle j (j = 1,2), respectively, and d is the impact parameter. From Eq. (1), it immediately follows that 300 eV H^+, H_2^+ or H_3^+ in anatase cannot cause Ti defects and the oxygen defect production is ineffective. The main production process of Ar ions is due to electron impact ionization of Ar,[38] however, the amount of electrons is heavily quenched along the tube.[40,41] The main ion species left are ArH^+ ions,[38,40–42] which can produce Ti and O vacancies effectively.

In order to estimate the energy of the incident ions, the mean free path (λ_1) of ArH^+ in a gas mixture composed of (neutral) Ar/H/H_2 has to be calculated as follows:[43]

$$\lambda_1 = \frac{1}{n_1\pi\sigma_{11}^2\sqrt{2} + \sum_i n_i\pi\sigma_{1i}^2\sqrt{1+m_1/m_i}}, \tag{2}$$

with

$$n_i = \frac{N_A P_i}{RT}, \tag{3}$$

where $\sigma_{12} = (\sigma_1 + \sigma_2)/2$ (averaged radii), m_i is the molecular mass of species i, P_i is the partial pressure, N_A is the Avogadro constant and R denotes the universal gas constant. The first term corresponds to the ArH^+–ArH^+ interaction and can be neglected, because the scattering cross section of ions is very low (Coulomb repulsion) and thus do not cause loss processes.[38] Using the aforementioned experimental parameters, a mean free path for ArH^+ in Ar/H/H_2 gas of $\lambda_1 \approx 2.41$ cm was found, before the recombination to atomic Ar occurs, where it was assumed all hydrogen atoms are bounded as ArH^+. Due to the large partial pressure, the main scattering occurs with Ar atoms. Considering

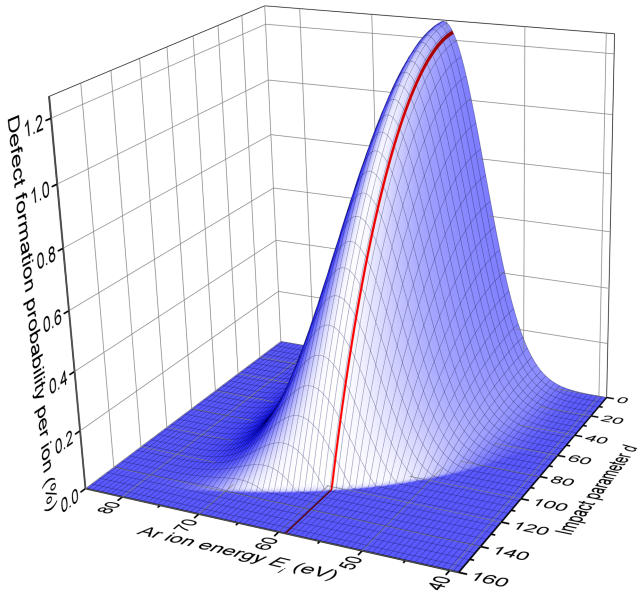

FIG. 2. The Ti defect formation probability (DFP) as a function of incident ion energy and impact parameter d. The red line indicates the mean ion energy E_i = 59.2 eV. The fraction of ions having a probability to produce defects of less than 0 %, is not shown.

the geometry of our experimental setup (parallel plate configuration) most ArH^+ ions will have an energy of 60.2 eV, which is high enough to produce vacancies. Upon impact, the molecule will split and the most energy remains with Ar ion. The impact energy will have a broad distribution with many ions below and and above the average value. Therefore, a normal energy distribution will be used to calculate the probability to have energy $E_i(\lambda_i)$, where the fraction of ions without suffering from a collision is $\propto \exp(-x/\lambda_1)$.[44] With this, and using Eq. (1), the probability to have a $E_{\mathrm{PKA}}(d)$ can be calculated. The defect formation probability (DFP) can then be estimated:[45]

$$\mathrm{DFP}(E_{\mathrm{PKA}}) = \begin{cases} 0 & \text{if } E_{\mathrm{PKA}} \le E_d, \\ \frac{1}{\gamma}\left(E_{\mathrm{PKA}}^{\alpha} - E_d^{\alpha}\right) & \text{if } E_{\mathrm{PKA}} > E_d, \end{cases} \tag{4}$$

where α and γ are free parameters taken from Ref. 46 for anatase. The resulting DFP for Ti atoms in anatase can be seen in FIG. 2. The red line indicates the mean energy of 59.2 eV of the incident Ar ions. A larger energy transfer E_{PKA} is less probable, but results in a higher probability to produce defects and thus, one finds a DFP of 1.26 % per ion. The largest amount of the incident particles do not cause any Ti vacancy and can be neglected – only ions with a feasible DFP are shown in the figure. Further details regarding defect production will be given in Section III D.

The penetration depth of the argon ions can be estimated using a Monte Carlo simulation program (SRIM[47]). The amount and type of the produced vacancies were estimated with the application of recent molecular dynamic studies[46] done for low-energy incident particles.

III. RESULTS AND DISCUSSION

The PIXE results, see Table I, show that the amount of ferromagnetic impurities does not exceed the minimum detection limit. A very small amount of copper was detected in the as-grown and treated parts of the TiO_2 film. Using the minimum detection limit one can estimate the maximal possible magnetic moment due to magnetic contaminants. Magnetic moments of ≈ 0.66 μemu due to Fe, ≈ 0.26 μemu due to Ni and ≈ 0.53 μemu due to Co were obtained, resulting in a maximum total magnetic moment due to magnetic impurities of ≈ 1.45 μemu. The PIXE results do not show any difference between the as-prepared thin film and the sample after ArH^+ irradiation. Therefore, it can be stated that the change of the magnetic properties is a consequence of the irradiation with argon ions. The contamination of the STO substrate is given in μg/g, whereas the impurity level of the TiO_2 thin film is given for the complete film with an area of 0.196 cm^2.

Structure analysis was done using XRD. The result is shown in FIG. 3. Beside the peaks of the STO substrate, only anatase peaks of (001) planes are found, indicating a perfect (001) orientation and an epitaxial growth of our films.[37] From the analysis of the peak positions, one finds a lattice constant $c \approx 9.61$ Å, which is slightly larger than the literature value of 9.51 Å for bulk TiO_2. After the irradiation with argon ions the X-ray diffraction was measured again and the position and width of the diffraction peaks showed no difference within experimental resolution.

A. Magnetic characteristics of the as-prepared thin films

The contribution of the (STO) substrate to the temperature dependence of magnetization has to be subtracted from the measurement including the thin film. For this aim, the temperature dependent magnetic moment of the STO (001) substrate alone, before deposition of the TiO_2 film, at a field of $\mu_0 H = 0.25$ T applied parallel and perpendicular to the c-axis, were measured. An example is shown

TABLE I. Results of PIXE measurement of the STO substrate and TiO_2 thin film. The total mass of TiO_2 film is ≈ 11.2 μg.

Element	Conc. in STO (μg/g)	Mass in TiO_2 film (ng)
Cr	< 7	< 2.5
Fe	< 6	< 3.1
Ni	< 7	< 4.3
Cu	11 ± 4	7.6 ± 2.8

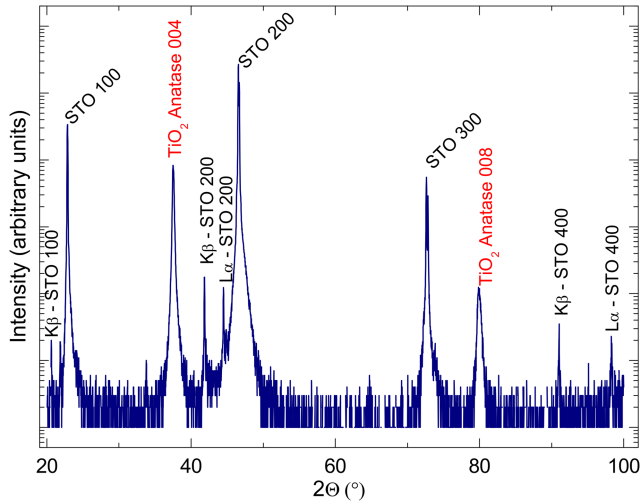

FIG. 3. The X-ray diffraction $\omega - 2\Theta$ scan of the as-grown TiO_2 thin film. Beside the anatase peaks in (001) direction, only the peaks of the STO substrate are visible.

in FIG. 4. The data were fitted using two contributions,

$$m(T) = m_d + C\mu_0 H/T, \tag{5}$$

where m_d accounts for the diamagnetic contribution, which one assumes to be temperature independent, and the second term is the paramagnetic Curie law, where C is the Curie constant. FIG. 4 shows that this model fits very well the obtained experimental results. The paramagnetic contribution is negligible at temperatures $T \geq 100$ K. The (temperature independent) diamagnetic contribution was $m_d \approx -17.2$ μemu at $\mu_0 H = 0.25$ T. The same field strength was used for the temperature dependent measurements with the TiO_2 film.

The zero-field-cooled (ZFC) and field-cooled (FC) measurements of the TiO_2 thin film are shown in FIG. 5, where the contribution of the STO substrate has been subtracted. To calculate the magnetization of the as-prepared thin film, a thickness of 150 nm was used. To calculate the magnetization of the treated films, a thickness of 2.5 nm was assumed, according to the penetration depth of the low-energy argon ions obtained by SRIM, see inset in FIG. 1.

In FIG. 6 the field hysteresis for the TiO_2 thin film at three different temperatures is shown for the as-prepared state as well as after the first and second irradiation. The contribution of the STO substrate was subtracted from the data. For the as-prepared state, a small magnetic moment with ferromagnetic behavior, see Figs. 5(a) and 6(a), was found; the values are close to the resolution limit of our SQUID device. It has been shown that ferromagnetism in doped and undoped TiO_2 strongly depends on lattice defects.[19,24,48–51] In our case such defects might have been introduced during the growth process, especially at the STO/TiO_2 interface as a consequence of the lattice mismatch

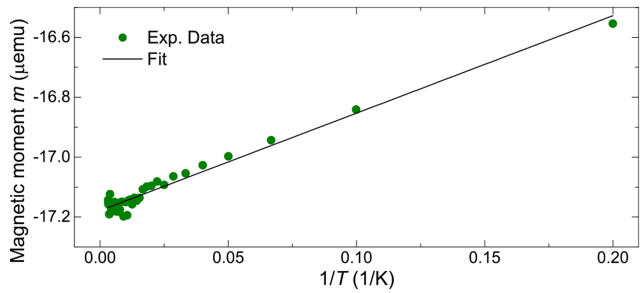

FIG. 4. Magnetic moment of the STO (001) substrate with an external field of $\mu_0 H = 0.25$ T applied parallel to the c-axis. The line was fitted using Eq. (5). C was found to be 1.3×10^{-5} (emuK/T).

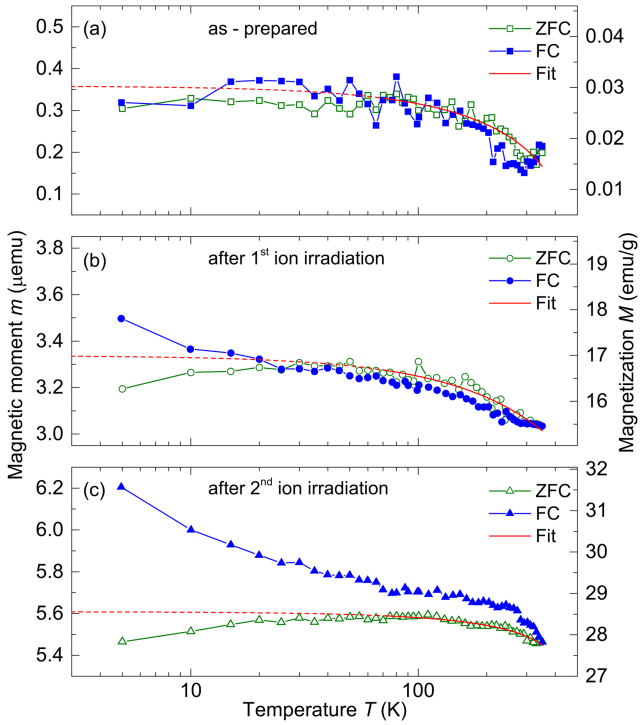

FIG. 5. Magnetic moment m (left y-axis) and magnetization M vs. temperature for the TiO_2 thin film in the (a) as-prepared state, (b) after the first and (c) after the second ion irradiation. The background signal of the substrate has been subtracted. The applied field was 0.25 T normal to the surface of the film.

($\approx 3.4\%$ for STO/anatase). As a result of the lattice stress at the interface, defects can be produced and they might be the reason for the initial ferromagnetic behavior in our sample. In addition, the initial FM contribution could be also originated from small amounts of magnetic contaminants, which maximum possible magnetic moment was estimated before. The magnetic moment of the as-prepared sample at low temperatures ($m_{0,ap} \approx 0.32$ μemu) will be subtracted from the data of the argon ion irradiated samples.

In order to estimate the FM Curie temperature, the mean field approximation[52]

$$m_{\mathrm{MFT}}(T) = m_0\left(1 - \frac{T}{T_{\mathrm{C}}}\right)^{\beta} \tag{6}$$

was used, where m_0 is the spontaneous magnetic moment at T = 0 K, T_{C} is the Curie temperature and β a critical exponent, which is predicted to be 1/2. This approximation (Eq. (6)) has been used to fit the high temperature dependence of the ZFC curves, see FIG. 5. For the as-prepared measurement, a Curie temperature of $T_{\mathrm{C}} \approx 445$ K and a critical exponent $\beta = 0.5$ were obtained, similar values have already been reported in the literature for both, T_{C} and β in TiO_2 thin films.[20]

B. Magnetic characteristics after the first irradiation

After the first ArH^+ irradiation ($\approx 28.6 \times 10^{16}$ argon ions/cm^2, flux: 1.59×10^{14} cm^{-2}s^{-1}), the magnetic moment increased to $m_0 \approx 3.5$ μemu, which is one order of magnitude larger than the as-prepared film and, after background subtraction, $\Delta m_{1st} \approx 3.2$ μemu, see Figs. 5 (b) and 6 (b). One observes not only an increase in the saturated magnetic moment but also in the coercive field, i.e. $H_c \approx 100$ Oe at all temperatures.

Applying the aforementioned MFT model to the results obtained after first ArH^+ irradiation, yields an effective critical exponent of $\beta \approx 0.17$ and a rough estimation of the Curie temperature of $T_{\mathrm{C}} \simeq 792$ K. Similar values have been found in defected TiO_2 thin films grown in a reduced

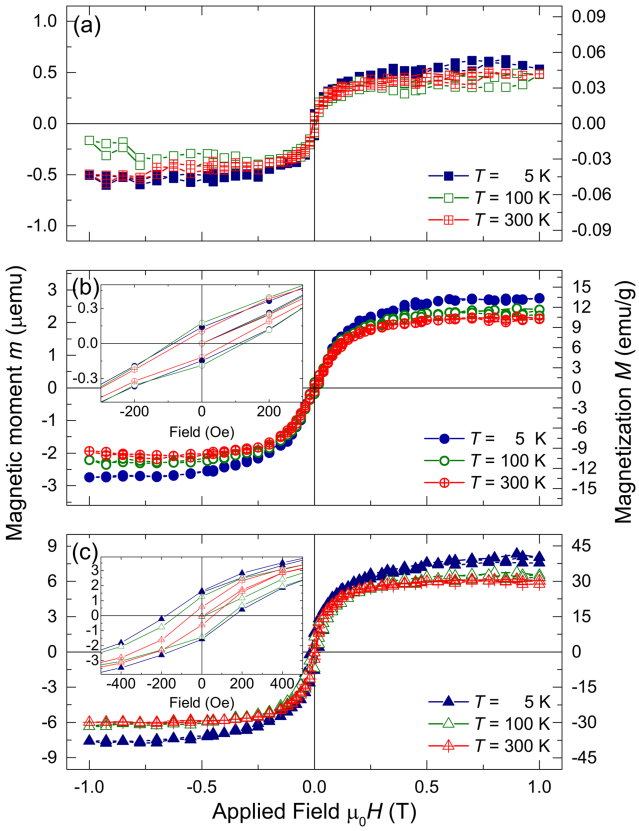

FIG. 6. Hysteresis measurements for (a) the as-prepared TiO_2 thin film, (b) the film after the first and (c) after the second ion irradiation. The paramagnetic contribution has been subtracted.

oxygen atmosphere[20] (T_C = 880 K). It is evident that there is only a small temperature dependence of the magnetization at saturation (within the measured temperature range), indicating that the Curie temperature is larger than room temperature. In FIG. 7 the remanence of the TiO_2 thin films after the first (and second) treatment is shown. Measurements of the as-prepared thin film did not show any remanent signal. After the first treatment, a remanence of $m_R \approx 0.4$ μemu at a temperature of T = 5 K was measured. The results show typical ferromagnetic behavior in the hysteresis and the temperature dependence of the remanence.

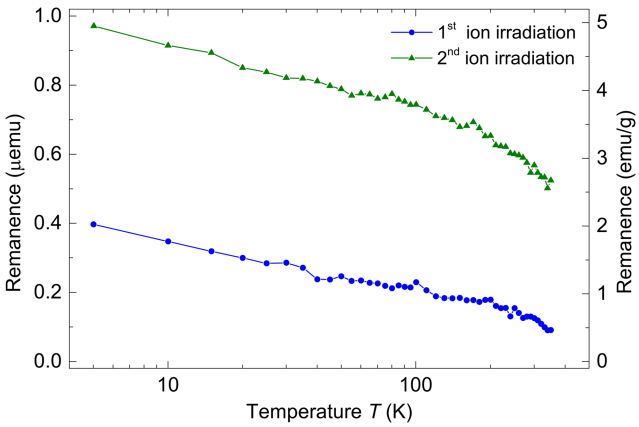

FIG. 7. Results of remanence measurements for TiO_2 thin film after the first and second Ar ion irradiation.

C. Magnetic characteristics after the second irradiation

In the second treatment, the amount of irradiated ions is twice the amount implanted during the first treatment (i.e. $\approx 57.3 \times 10^{16}$ argon ions/cm^2). The temperature dependent measurements can be seen in FIG. 5. Now a magnetic moment (at 0.25 T and T = 5 K) of $m_0 \approx 6.2$ μemu is obtained, and $\Delta m_{2nd-ap} \approx 5.9$ μemu, with a reduced Curie temperature of $T_C \simeq 473$ K. Considering the produced magnetic moment after the first irradiation of $\Delta m_{1st} \approx 3.2$ μemu, one would expect a magnetic moment of 9.6 μemu. Therefore, the observed increase is ≈ 0.6 times less than one would expect from the first treatment, if there was a linear relation with the amount of introduced ions. This indicates that, the amount of formed local magnetic moments scales not linearly with the argon ions fluence and that the magnetic defect formation probability is not only a function of crystallographic direction, PKA energy and temperature, but also depends on the defect concentration, until saturation occurs. Similar behavior was already observed for DIM.[34,35]

In FIG. 7 the temperature dependence of the remanence of the TiO_2 thin film after the second Ar ion irradiation is shown. The temperature dependence shows a stronger variation, as was already observed in ZFC – FC curves, with a remanence of $m_R \approx 0.98$ μemu at a temperature of T = 5 K. Considering the PIXE and the remanence results, one can discard the possibility that the ferromagnetic order originates from impurities. The coercive field increased to $H_c \approx 180$ Oe at T = 5 K but it decreases to $H_c \approx 50$ Oe at T = 300 K. These results are in agreement with the temperature dependence of the magnetic moment (ZFC–FC) and remanence measurements. The observed change between the first and second treatment cannot be attributed to aging effects because measurements were reproducible when the sample was investigated again after several weeks. After the second Ar ion irradiation one finds a maximum magnetization of $M \approx 40$ emu/g. This value was calculated using the complete area of the film. However, assuming the formation of clusters rather than a uniform distribution,[46] would result in a higher magnetization.

D. Origin of the defect induced magnetic moment

Heavy or high energy ions create dense collision subcascades with dynamic annealing with only few reordering.[53] Furthermore, these regions may lose their chemical order resulting in amorphous pockets,[54,55] which are resistant to reordering. However, light or low-energy ions produce dilute vacancy-interstitial pairs – Frenkel pairs (FPs) – along the ion path and/or upon collision. Due to diffusing ions and mobile vacancies, recombination processes are very likely and chemical reordering takes places.[35,53] Thus, TRIM results are usually poor at low incident ion energy.[46] Besides, the displacement energy should be considered as a function of chemical composition, which results in different E_d values for rutile, anatase and brookite, as experiments on the polymorphisms of TiO_2 demonstrate.[45,46]

Because defects as the FP are not in general stable,[45,46,56,57] a way to estimate a stable defect concentration is done through the introduction of the defect formation probability (DFP).[56] The DFP depends on the crystallographic direction, the energy E_{PKA} and temperature. As soon as E_{PKA} reaches the threshold displacement energy, the probability to produce defects increases with energy, resulting in a smooth, non-linear increment as a result of recombination of unstable Frenkel pairs. A piecewise power law can be used to describe the behavior, see Eq. (4). Temperature has a large influence on E_d; calculations indicate that E_d increases for oxygen from 18 eV at 300 K to 53 eV at 750 K due to activated recombination.[56] To our best knowledge, experimental studies of E_d for anatase have not been reported yet. In the case of rutile, values between 45 eV and 50 eV for Ti and 33 eV for oxygen were reported using TEM.[58]

Molecular dynamic studies have shown that for low PKA energies, ≈ 75 % of the produced defects are Ti vacancies,[46] and for anatase at room temperature, a Frenkel pair (Ti_V + Ti_I) results in recombination and is stable only when a second FP is produced at the nearest neighbouring sites, indicating that stability is only possible due to the localization of two FPs (di-FP).[46,59] Simulations[45] and time-resolved cathodoluminescence spectroscopy[60] show that at room temperature the recombination processes reduce the amount of stable oxygen defects. Furthermore, oxygen defected TiO_2 is known to interact with the ambient air[61] such that recombination occurs. However, the sample was measured several weeks after irradiation and no change of the magnetic moment was observed.

TABLE II. Summary of different parameters and results of the TiO_2 thin film after first and second argon ion irradiation. Employing the results of molecular dynamic simulations[46] yields a magnetic moment per Ti divacancy $m_{di-FP}(\mu_B)$.

	$1^{st}ArH^+$ treatment	$2^{nd}ArH^+$ treatment
Nr. of ArH^+	5.6×10^{16}	1.12×10^{17}
Flux	$1.59\times10^{14}cm^{-2}s^{-1}$	
$m_{di-FP}(\mu_B)$	2.01 per di-Ti_V	1.3 per di-Ti_V

In addition, theoretical work predicts that the density of states in an oxygen deficient system is not spin polarized and that there are no magnetic moments at the O vacancies.[28]

Following these experimental and theoretical results, one concludes that the magnetic moment generated at the titanium di-FPs. Ti vacancies as a origin of FM were already found for as-prepared $Ti_{0.905}O_2$[25] and TiO_2 irradiated by 4 MeV Ar^{5+}.[27] Theoretical work predicts a magnetic moment per Ti vacancy of 3.5 μ_B. When a Ti vacancy is created, holes are introduced into the O-2*p* π band. Exchange splitting due to spin polarization of the low energy majority-spin state and high energy minority-spin state, lowers the total energy in the presence of holes. When two Ti atoms are removed from the nearest neighbouring sites, an oxygen dimer is formed along the *z*-direction.[28] The 2 π^* electrons of the oxygen dimer will drop to the lower states and compensate the holes. In addition, two Ti-O bonds are broken. This leads to a further decrease of the magnetic moment of the di-FP down to 2 μ_B per Ti divacancy.[28] The probability to produce a Ti di-FP is ≈ 24.4 % per defect.[46] Therefore, considering the effective DFP of 1.26 % (see Section II B), a magnetic moment of $m = 2.01$ μ_B per Ti di-vacancy is obtained. This result (see Table II) agrees very well with that of Peng et al.[28] (2 μ_B per di−FP). Further experimental parameters are given in Table II.

After the second Ar ion irradiation, and using the same DFP, the magnetic moment per Ti divacancy reduces to $m = 1.3$ μ_B. This implies that the transformation to the ferromagnetic state saturates and less magnetic defects are produced increasing the defect.[34,35] The mechanism can be regarded as ferromagnetic super exchange mechanism, similar to the Hubbard model.[28,62] The more pronounced temperature dependence can be attributed to reduced long-range magnetic coupling as the defect concentration, and the disorder, increases reducing hybridization and the Curie temperature.

E. Unusual magnetic anisotropy at low defect concentration

An unusual magnetic anisotropy was reported for defective HfO_2[9] and Cr doped TiO_2[63] thin films, i.e. the magnetization at applied fields normal to the surface of the film reaches its saturation at much smaller fields than for the parallel direction, in contrast to the expected magnetic form anisotropy. In order to verify the possibility of such an anisotropy in the TiO_2 films, measurements

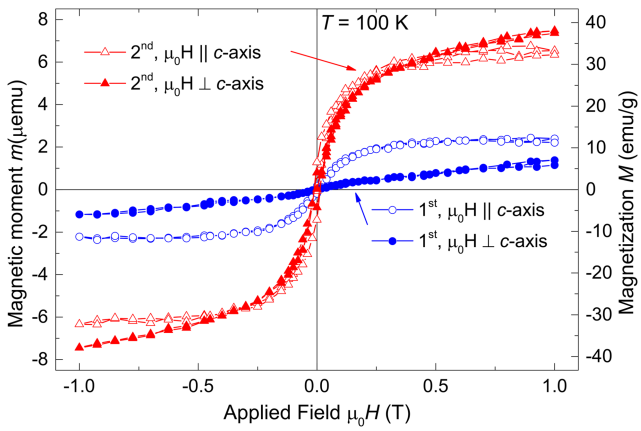

FIG. 8. Anisotropy of the saturated magnetization after first and second argon ion irradiation at a temperature of $T = 100$ K. After first treatment, an easy axis perpendicular to the film surface can be observed.

under an applied field normal to the *c*-axis of the thin film were performed. For comparison, FIG. 8 shows the results of the hysteresis curves at $T = 100$ K under an applied field parallel and perpendicular to the *c*-axis. A clear anisotropy of the saturated magnetic moment after the first Ar ion irradiation is observed, similar to what has been already observed in the literature for dilute semiconductor thin films.[9,34,63] The results show that the magnetization caused by irradiation of argon ions has a defined easy axis parallel to the *c*-axis, i.e. normal to the film surface. After the second treatment this magnetic anisotropy practically vanished, indicating that a preserved atomic lattice with a not very large defect concentration is required to get this interesting anisotropy. This anisotropy and the way to produce it may have useful applications for memory devices. Future studies should consider the possibility to produce well defined magnetic moments pinned normal to the main surface by single Ar ion irradiation, using, for example, nano-implanters.[64]

IV. SUMMARY

Epitaxial anatase TiO_2 thin films were grown by PLD on STO substrates. Their phase and the crystallographic orientation were confirmed using X-ray diffraction measurements. The impurities concentration of the samples were examined using PIXE. Their concentration was too low to be the origin of the measured ferromagnetic signals. The as-grown sample shows a small ferromagnetic signal without magnetic anisotropy and with a Curie temperature of $T_C \approx 445$ K. The origin of this magnetic signal is probably related to lattice mismatch induced defects or defects generated during the growth process. The experimental studies presented in this work show a simple way to induce magnetism in anatase TiO_2 thin films, via irradiation of low energy ions. After the first irradiation, the magnetic moment at saturation increased by one order of magnitude, showing a very high Curie temperature of $T_C \approx 792$ K. A considerable out-of-plane magnetic anisotropy in the magnetization has been found. After the second irradiation, the magnetic moment increased again, but not linearly with the ion fluence, whereas T_C was reduced and the anisotropy vanished. Experimental[24–27] and theoretical[28,45,46,56,57] results show that oxygen vacancies are not the source of magnetic moments, but Ti vacancies. The used ion energy to produce the defects triggers the formation of Ti di-vacancies or di-vacancy clusters.[45,46] The obtained magnetic moment per Ti di-FP of $m \approx 2\ \mu_B$ agrees with literature reports.[28] The triggered magnetization at low ion energies and fluences shows an interesting anisotropy with an easy axis perpendicular to the film surface. The above mentioned experimental results offer new possibilities for future applications of DIM in TiO_2 thin films, using low-energy ion irradiation which can be easily included in industrial processes.

ACKNOWLEDGMENTS

This work was supported by DFG through the Collaborative Research Center SFB 762 "Functionality of Oxide Interfaces" and the University Leipzig within the program of Open Access Publishing. We thank Holger Hochmuth for the PLD growth of the TiO_2 thin films.

[1] P. Esquinazi, W. Hergert, D. Spemann, A. Setzer, and A. Ernst, "Defect-induced magnetism in solids." *IEEE Trans. on Magn.* **49**, 4668–4674 (2013).
[2] A. Sundaresan and C. N. R. Rao, "Ferromagnetism as a universal feature of inorganic nanoparticles," *Nano Today* **4**, 96–106 (2009).
[3] C. D. Pemmaraju and S. Sanvito, "Ferromagnetism driven by intrinsic point defects in HfO_2," *Phys. Rev. Lett.* **94**, 217205 (2005).
[4] J. M. D. Coey, M. Venkatesan, and C. B. Fitzgerald, "Donor impurity band exchange in dilute ferromagnetic oxides," *Nature Materials* **4**, 173–179 (2005).
[5] D. Sanyal, M. Chakrabarti, T. K. Roy, and A. Chakrabarti, "The origin of ferromagnetism and defect-magnetization correlation in nanocrystalline ZnO," *Phys. Lett. A* **371**, 482–485 (2007).
[6] N. Kumar, D. Sanyal, and A. Sundaresan, "Defect induced ferromagnetism in MgO nanoparticles studied by optical and positron annihilation spectroscopy," *Chem. Phys. Lett.* **477**, 360–364 (2009).
[7] S. Zhou, E. Cižmár, K. Potzger, M. Krause, G. Talut, M. Helm, J. Fassbender, S. A. Zvyagin, J. Wosnitza, and H. Schmidt, "Origin of magnetic moments in defective TiO_2 single crystals," *Phys. Rev. B* **79**, 113201 (2009).
[8] S. A. Wolf, D. D. Awschalom, R. A. Buhrman, J. M. Daughton, S. von Molnár, M. L. Roukes, A. Y. Chtchelkanova, and D. M. Treger, "Spintronics: A spin-based electronics vision for the future," *Science: Mag. and Mat.,* **294**, 1488–1495 (2001).
[9] M. Venkatesan, C. B. Fitzgerald, and J. M. D. Coey, "Unexpected magnetism in a dielectric oxide," *Nature,* **430**, 630 (2004).
[10] J. M. D. Coey, M. Venkatesan, P. Stamenov, C. B. Fitzgerald, and L. S. Dorneles, "Magnetism in hafnium dioxide," *Phys. Rev. B,* **72**, 024450 (2005).

[11] J. Zippel, M. Lorenz, A. Setzer, M. Rothermel, D. Spemann, P. Esquinazi, M. Grundmann, G. Wagner, R. Denecke, and A. A. Timopheev, "Defect-induced magnetism in homoepitaxial manganese-stabilized zirconia thin films," *J. Phys. D: Appl. Phys.,* **46**, 275002 (2013).
[12] J. Zippel, M. Lorenz, A. Setzer, G. Wagner, N. Sobolev, P. Esquinazi, and M. Grundmann, "Defect-induced ferromagnetism in undoped and Mn-doped zirconia thin films," *Phys. Rev. B,* **82**, 125209 (2010).
[13] A. Sundaresan, R. Bhargavi, N. Rangarajan, U. Siddesh, and C. N. R. Rao, "Ferromagnetism as a universal feature of nanoparticles of the otherwise nonmagnetic oxides," *Phys. Rev. B,* **74**, 161306 (2006).
[14] Q. Xu, H. Schmidt, S. Zhou, K. Potzger, M. Helm, H. Hochmuth, M. Lorenz, A. Setzer, P. Esquinazi, C. Meinecke, and M. Grundmann, "Room temperature ferromagnetism in ZnO films due to defects," *Appl. Phys. Lett.,* **92**, 082508 (2008).
[15] M. Khalid, M. Ziese, A. Setzer, P. Esquinazi, M. Lorenz, H. Hochmuth, M. Grundmann, D. Spemann, T. Butz, G. Brauer, W. Anwand, G. Fischer, W. A. Adeagbo, W. Hergert, and A. Ernst, "Defect-induced magnetic order in pure ZnO films," *Phys. Rev. B,* **80**, 035331 (2009).
[16] I. Lorite, B. Straube, H. Ohldag, P. Kumar, M. Villafuerte, P. Esquinazi, C. E. Rodríguez Torres, S. Perez de Heluani, V. N. Antonov, L. V. Bekenov, A. Ernst, M. Hoffmann, S. K. Nayak, W. A. Adeagbo, G. Fischer, and W. Hergert, "Advances in methods to obtain and characterise room temperature magnetic zno," *Appl. Phys. Lett.,* **106**, 082406 (2015).
[17] J. M. D. Coey, "d^0 ferromagnetism," *Sol. State Sci.,* **7**, 660–667 (2005).
[18] D.-X. Li, X.-B. Qin, L.-R. Zheng, Y.-X. Li, X.-Z. Cao, Z.-X. Li, J. Yang, and B.-Y. Wang, "Defect types and room-temperature ferromagnetism in undoped rutile TiO_2 single crystals," *Chin. Phys. B,* **22**(3), 037504 (2013).
[19] N. H. Hong, J. Sakai, N. Poirot, and V. Brizé, "Room-temperature ferromagnetism observed in undoped semiconducting and insulating oxide thin films," *Phys. Rev B,* **73**, 132404 (2006).
[20] S. D. Yoon, Y. Chen, A. Yang, T. L. Goodrich, X. Zuo, K. Ziemer, C. Vittoria, and V. G. Harrisa, "Magnetic semiconducting anatase $TiO_{2-\delta}$ grown on (100) $LaAlO_3$ having magnetic order up to 880 k," *J. of Magn. and mag. Mat.,* **309**, 171–175 (2007).
[21] H. Thakur, P. Thakur, R. Kumar, N. B. Brookes, K. K. Sharma, A. P. Singh, Y. Kumar, S. Gautam, and K. H. Chae, "Irradiation induced ferromagnetism at room temperature in TiO_2 thin films: X-ray magnetic circular dichroism characterizations," *Appl. Phys. Lett.,* **98**, 192512 (2011).
[22] M. M. Cruz, R. C. da Silva, N. Franco, and M. Godinho, "Ferromagnetism induced in rutile single crystals by argon and nitrogen implantation," *J. Phys.: Condens. Matter,* **21**, 206002 (2009).
[23] S. D. Yoon, Y. Chen, A. Yang, T. L. Goodrich, X. Zuo, D. A. Arena, K. Ziemer, C. Vittoria, and V. G. Harris, "Oxygen-defect-induced magnetism to 880 k in semiconducting anatase $TiO_{2-\delta}$ films," *J. Phys.: Condens. Matter,* **18**, L355–L361 (2006).
[24] A. K. Rumaiz, B. Ali, A. Ceylan, M. Boggs, T. Beebe, and S. I. Shah, "Experimental studies on vacancy induced ferromagnetism in undoped TiO_2," *Solid State Comm.,* **144**, 334–338 (2007).
[25] Q. Zhao, P. Wu, B. L. Li, Z. M. Lu, and E. Y. Jiang, "Activation of room-temperature ferromagnetism in nonstoichiometric $TiO_{2-\delta}$ powders by oxygen vacancies," *Jour. Appl. Physics,* **104**, 073911 (2008).
[26] S. Wang, L. Pan, J.-J. Song, W. Mi, J.-J. Zou, L. i Wang, and X. Zhang, "Titanium-defected undoped anatase TiO_2 with p-type conductivity, room-temperature ferromagnetism, and remarkable photocatalytic performance," *J. of Amer. Chem. Soc.,* **137**, 2975–2983 (2015).
[27] D. Sanyal, M. Chakrabarti, P. Nath, A. Sarkar, D. Bhowmick, and A. Chakrabarti, "Room temperature ferromagnetic ordering in 4 mev Ar^{5+} irradiated TiO_2," *J. Phys. D,* **47**, 025001 (2014).
[28] H. Peng, J. Li, S.-S. Li, and J.-B. Xia, "Possible origin of ferromagnetism in undoped anatase TiO_2," *Phys. Rev. B,* **79**, 092411 (2009).
[29] K. Piao, D. Li, and D. Wei, "The role of short exchange length in the magnetization processes of $L1_0$-ordered FePt perpendicular media," *J. of Magnetism and Magnetic Materials,* **303**, e39–e43 (2006).
[30] C. T. Rettner, S. Anders, J. E. E. Baglin, T. Thomson, and B. D. Terris, "Characterization of the magnetic modification of Co/Pt multilayer films by He+, Ar+ and Ga+ ion irradiation," *Appl. Phys. Lett.,* **80**, 279 (2002).
[31] K. Dörr, "Ferromagnetic manganites: Spin-polarized conduction versus competing interactions," *J. Phys. D: Appl. Phys.,* **39**, R125–R150 (2006).
[32] M. Abes, J. Venuat, D. Muller, A. Carvalho, G. Schmerber, E. Beaurepaire, A. Dinia, and V. Pierron-Bohnes, "Magnetic patterning using ion irradiation for highly ordered CoPt alloys with perpendicular anisotropy," *J. of Appl. Phys.,* **96**, 7420 (2004).
[33] T. Devoldera, C. Chapperta, and H. Bernas, "Theoretical study of magnetic pattern replication by He+ ion irradiation through stencil masks," *J. of Magnetism and Magnetic Materials,* **249**, 452–457 (2002).
[34] D. G. Merkel, L. Bottyán, F. Tanczikó, Z. Zolnai, N. Nagy, G. Vértesy, J. Waizinger, and L. Bommer, "Magnetic patterning perpendicular anisotropy FePd alloy films by masked ion irradiation," *J. of Appl. Phys.,* **109**, 124302 (2011).
[35] J. Fassbender, M. O. Liedke, T. Strache, W. Möller, E. Menéndez, J. Sort, K. V. Rao, S. C. Deevi, and J. Noqués, "Ion mass dependence of irradiation-induced local creation of ferromagnetism in $Fe_{60}Al_{40}$ alloys," *Phys. Rev. B,* **77**, 174430 (2008).
[36] E. P. Houwman, G. Maris, G. M. De Luca, N. Niermann, G. Rijnders, D. H. A. Blank, and S. Speller, "Out-of-plane magnetic domain structure in a thin film of $La_0.67Sr_0.33MnO_3$ on $SrTiO_3$ (001) observed by magnetic force microscopy," *Phys. Rev. B,* **77**, 184412 (2008).
[37] M. Kneiß, M. Jenderka, K. Brachwitz, M. Lorenz, and M. Grundmann, "Modeling the electrical transport in epitaxial undoped and Ni-, Cr-, and W-doped TiO_2 anatase thin films," *Appl. Phys. Lett.,* **105**, 062103 (2014).
[38] A. Bogaerts and R. Gijbels, "Hybrid monte carlo-fluid modeling network for an argon/hydrogen direct current glow discharge," *Spectrochimica Acta Part B,* **57**, 1071–1099 (2002).
[39] Husinsky, *Modellbildung in der physik*. University Lecture, see Eq. (7.22) in chapter 7, 2013. URL https://vowi.fsinf.at/wiki/Datei:TU_Wien-Modellbildung_in_der_Physik_VU_(Husinsky)_-_PausPhysik-Kapitel7-St%C3%B6%C3%9Fe.pdf.

[40] R. F. G. Meulenbroeks, R. A. H. Engeln, M. N. A. Beurskens, R. M. J. Paffen, M. C. M. van de Sanden, J. A. M. van der Mullen, and D. C. Schram, "The argon-hydrogen expanding plasma: model and experiments," *Plasma Sources Sci. Technol.,* **4**, 74–85 (1994).
[41] R. F. G. Meulenbroeks, A. J. van Beck, A. J. G. van Helvoort, M. C. M. van de Sanden, and D. C. Schram, "Argon-hydrogen plasma jet investigated by active and passive spectroscopic means," *Phys. Rev. E,* **49**, 4397 (1994).
[42] R. S. Mason, P. D. Miller, and I. P. Mortimer, "Anomalous loss of ionization in argon-hydrogen plasma studied by fast flow glow discharge mass spectrometry," *Phys. Rev. E,* **55**, 7462 (1997).
[43] S. Chapman and T. G. Cowling, *The Mathematical Theory of Non-uniform Gases: An Account of the Kinetic Theory of Viscosity, Thermal Conduction and Diffusion in Gases* (Cambridge Mathematical Library, 1970).
[44] S. K. Roy, *Thermal Physics and Statistical Mechanics* (New Age International, 2001).
[45] M. Robinson, N. A. Marks, and G. R. Lumpkin, "Sensitivity of the threshold displacement energy to temperature and time," *Phys. Rev. B,* **86**, 134105 (2012).
[46] M. Robinson, N. A. Marks, and G. R. Lumpkin, "Structural dependence of threshold displacement energies in rutile, anatase and brookite TiO_2," *Mat. Chem. and Phys.,* **147**, 311–318 (2014).
[47] J. F. Ziegler, "Stopping and range of ions in matter," *The Stopping and Range of Ions in Matter* (2013).
[48] T. C. Kaspar, S. M. Heald, C. M. Wang, J. D. Bryan, T. Droubay, V. Shutthanandan, S. Thevuthasan, D. E. McCready, A. J. Kellock, D. R. Gamelin, and S. A. Chambers, "Negligible magnetism in excellent structural quality $Cr_xTi_{1-x}O_2$ anatase: Contrast with high-T_c ferromagnetism in structurally defective $Cr_xTi_{1-x}O_2$," *Phys. Rev. Lett.,* **95**, 217203 (2005).
[49] S. Duhalde, M. F. Vignolo, F. Golmar, C. Chiliotte, C. E. R. Torres, L. A. Errico, A. F. Cabrera, M. Rentería, F. H. Sánchez, and M. Weissmann, "Appearance of room-temperature ferromagnetism in Cu-doped TiO_{2-d} films," *Phys. Rev. B,* **72**, 161313 (2005).
[50] I. S. Elfimov, A. Rusydi, S. I. Csiszar, Z. Hu, H. H. Hsieh H.-J. Lin, C. T. Chen, R. Liang, and G. A. Sawatzky, "Magnetizing oxides by substituting nitrogen for oxygen," *Phys. Rev. Let.,* **98**, 137202 (2007).
[51] P. Mohantya, D. Kabiraj, R. K. Mandal, P. K. Kulriya, A. S. K. Sinha, and C. Ratha, "Evidence of room temperature ferromagnetism in argon/oxygen annealed TiO_2 thin films deposited by electron beam evaporation technique," *Jour. of Magn. and Magn. Mat.,* **355**, 240–245 (2014).
[52] L. P. Kadanoff, W. Gotze, D. Hamblen, R. Hecht, E. A. S. Lewis, V. V. P. Ciauskas, M. Rayl, and J. Swift, "Static phenomena near critical points: Theory and experiment," *Rev. of Mod. Phys.,* **39**, 395–429 (1967).
[53] R. S. Averback, R. Benedek, and K. L. Merkle, "Efficiency of defect production in cascades," *J. of Nucl. Mat.,* **69–70**, 786–789 (1978).
[54] M.-J. Caturla, T. Díaz de la Rubia, L. A. Marqués, and G. H. Gilmer, "Ion-beam processing of silicon at kev energies: A molecular-dynamics study," *Phys. Rev. B,* **54**, 16683 (1996).
[55] A. V. Krasheninnikov, K. Nordlund, and J. Keinonen, "Production of defects in supported carbon nanotubes under ion irradiation," *Phys. Rev. B,* **65**, 165423 (2002).
[56] M. Robinson, N. A. Marks, K. R. Whittle, and G. R. Lumpkin, "Systematic calculation of threshold displacement energies: Case study in rutile," *Phys. Rev. B,* **85**, 104105 (2012).
[57] B. S. Thomas, N. A. Marks, L. R. Corrales, and R. Devanathan, "Threshold displacement energies in rutile TiO_2: A molecular dynamics simulation study," *Nucl. Instr. and Methods Phys. Res. B,* **239**, 191–201 (2005).
[58] E. C. Buck, "Effects of electron irradiation of rutile," *Rad. Ef. and Def. in Sol.,* **133**, 141–152 (1995).
[59] H.-S. Ahn, S. Han, and C. S. Hwang, "Pairing of cation vacancies and gap-state creation in TiO_2 and HfO_2," *Appl. Phys. Lett.,* **90**, 252908 (2007).
[60] K. L. Smith, R. Cooper, M. Colella, and E. R. Vance, "Measured displacement energies of oxygen ions in zirconolite and rutile," *MRS Proceedings,* **663**, 373 (2000).
[61] U. Diebold, "The surface science of titanium dioxide," *Surf. Sci. Rep.,* **48**, 53–229 (2003).
[62] A. Mielke and H. Tasaki, "Ferromagnetism in the hubbard model," *Commun. Math. Phys.,* **158**, 341–371 (1993).
[63] J. Osterwalder, T. Droubay, T. Kaspar, J. Williams, C. M. Wang, and S. A. Chambers, "Growth of Cr-doped TiO_2 films in the rutile and anatase structures by oxygen plasma assisted molecular beam epitaxy," *Thin Solid Films,* **484**, 289–298 (2005).
[64] J. Meijer, S. Pezzagna, T. Vogel, B. Burchard, H. H. Bukow, I. W. Rangelow, Y. Sarov, H. Wiggers, I. Plümel, F. Jelezko, J. Wrachtrup, F. Schmidt-Kaler, W. Schnitzler, and K. Singer, "Towards the implanting of ions and positioning of nanoparticles with nm spatial resolution," *Appl. Phys. A,* **91**, 567–571 (2008).